frontiers | Frontiers in Chemistry

ORIGINAL RESEARCH
published: 13 June 2022
doi: 10.3389/fchem.2022.913874

Cu-Based Multicomponent Metallic Compound Materials as Electrocatalyst for Water Splitting

Peijia Wang†, *Jingjing An*†, *Zhenyu Ye*, *Wei Cai* and *Xiaohang Zheng**

School of Materials Science and Engineering, Harbin Institute of Technology, Harbin, China

In this study, Cu-based multicomponent metallic compound materials M-Cu (M = Mn, Fe, Co, Ni, and Pt) were studied as electrocatalytic materials for water splitting. Different metal materials attached to the copper foam substrate can change the valence states of copper and oxygen, resulting in the change of electronic structure of the materials, thus changing its catalytic activity.

Keywords: Cu-based materials, electronic structure, water splitting, valence states, multicomponent

Edited by:
Zhong Jin,
Nanjing University, China

Reviewed by:
Shouhua Feng,
Jilin University, China
Leilei Xu,
Nanjing University of Information Science and Technology, China
Weiwei Cai,
China University of Geosciences Wuhan, China
Dong-Sheng Li,
China Three Gorges University, China

****Correspondence:***
Xiaohang Zheng
zhengxiaohang@hit.edu.cn

†These authors have contributed equally to this work

Specialty section:
This article was submitted to Inorganic Chemistry, a section of the journal Frontiers in Chemistry

Received: *06 April 2022*
Accepted: *02 May 2022*
Published: *13 June 2022*

Citation:
Wang P, An J, Ye Z, Cai W and Zheng X (2022) Cu-Based Multicomponent Metallic Compound Materials as Electrocatalyst for Water Splitting. Front. Chem. 10:913874. doi: 10.3389/fchem.2022.913874

HIGHLIGHTS

- The M-Cu (M = Mn, Fe, Co, Ni, and Pt) samples were obtained by a facile method on the copper foam substrate.
- The good HER and OER performances come from the introduction of the second ions, which change the valence states of copper and oxygen elements, resulting in the change of electronic structure of the materials.

INTRODUCTION

Electrochemical processes such as water splitting are a promising method to alleviate energy and environmental problems (Zhang et al., 2017a; Anandhababu et al., 2018; Zhang et al., 2019a). However, the efficiency of anodic oxygen evolution (OER) is limited by its slow kinetics (Zhou et al., 2018; Sultan et al., 2019). At present, precious metal is still the best catalyst (Li et al., 2018); in order to reduce the consumption of precious metal, looking for cheap alternatives is the general trend.

Recently, the transition metallic compound has attracted a lot of attention due to their intrinsically enhanced safety and high availability through the conversion reaction (Kim et al., 2021; Zhang et al., 2021; Zhu et al., 2021). Among them, single-component metallic compound has also shown excellent behavior as an electrocatalyst for water splitting (Jebaslinhepzybai et al., 2021). In particular, the introduction of the second metal ions can change the electronic state of the active metal, vacancy concentration (Yuan et al., 2021), coordination environment, or electron band structure (Zhang et al., 2017b), therefore enhancing HER kinetics (Yang and Chen, 2020; Li et al., 2021), such as the use of plasma treatment method to activate the Cu surface (Lee et al., 2018; Tomboc et al., 2020), by doping additional elements or with other metal alloys to adjust the binding energy of the reaction intermediates (Gatalo et al., 2019), and the Cu species into a specific structure or a specific crystal plane (Koh and Strasser, 2007; Liu et al., 2021; Yan et al., 2021; Yang et al., 2021). Christoph R. Muller (Kuznetsov et al., 2020) studied the surface oxygen vacancies (V_O) in $Y_{1.8}M_{0.2}Ru_2O_{7-\delta}$ (M = Cu, Co, Ni, Fe, Y) by an increased concentration of V_O sites correlating with a superior OER activity. These studies show that not only the dispersion of metal particles but also the properties of the substrate can alter the electronic states and chemical properties of the active site (Zhu et al., 2017), thus altering the catalytic activity (Yan et al., 2020; Zhang et al., 2020; Qiu et al.,

2021; Wu et al., 2021). However, obtaining a catalyst of high activity remains a huge challenge. Therefore, it is necessary to design a new strategy for Cu-based catalysts.

Herein, M-Cu (M = Mn, Fe, Co, Ni, and Pt) multicomponent metallic compound materials are studied as electrocatalytic materials for water splitting. Different metal materials attached to the copper foam substrate can change the valence states of copper and oxygen, resulting in the change of electronic structure of the materials, thus changing its catalytic activity. As a result, for non-precious metal, the overpotentials for the Co–Cu sample at a current density of 10 mA/cm^2 were 207.0 mV for OER and 329.8 mV for HER in 1 M KOH. Moreover, when adding the precious metal Pt, the high OER and HER catalytic efficiencies were also observed in the Pt–Cu sample.

EXPERIMENTAL SECTION

The Cu foam was purchased from Jia Yisheng Co., Ltd. (Kun Shan); the thickness is 1.5mm, the surface density is 600 g/m^2, and the hole number is 110 ppi. Firstly, the copper foam was cut into 2 cm × 2 cm sized squares and soaked in hydrochloric acid (deionized water: hydrochloric acid = 3:1) using an ultrasonic cleaner for 30 s.

Then, they were immersed in an equimolar solution of $FeCl_3$ (0.6 g per 30 ml), $CoCl_2$, $NiCl_4$, $MnCl_2$, and chloroplatinic acid solution for 30 min, separately. Finally, they were taken out and allowed to dry using a hair dryer.

MATERIAL CHARACTERIZATION

The morphologies of the products were investigated by field-emission scanning electron microscopy (SEM, Helios Nanolab 600i), transmission electron microscope (TEM, Tecnai G2 F30), X-ray diffraction (XRD, D8 Advance), and X-ray photoelectron spectroscopy (XPS, Thermo Fisher).

ELECTROCHEMICAL TEST

All electrochemical performances were measured in the electrochemical workstation (CHI 760E). The HER and OER properties were measured in a three-electrode system, and the obtained samples, Hg/HgO, and carbon rod were used as working electrode, reference electrode and counter electrode, respectively. The electrolyte was 1.0 M KOH solution. All the potential was converted to RHE. LSV tests were carried out at a scan rate of 2 mV/s. The EIS measurement was carried out in a frequency range from 0.1 Hz to 100 kHz.

RESULTS AND DISCUSSION

In this work, the M-Cu (M = Mn, Fe, Co, Ni, and Pt) samples were achieved by a facile method; the surface morphology of the pristine samples was investigated by SEM. As shown in **Figure 1**, combining the SEM-mapping analysis (**Supplementary Figure S1**), the simple electron microscopic diagram proves that the whole foam copper is covered by the sample.

X-ray diffraction (XRD) analysis is employed to confirm the crystal structure of the as-synthesized M-Cu samples. It can be seen from **Supplementary Figure S2** that the M-Cu samples were located at 43.3, 50.4, and 74.1°,corresponding to (111), (200), and (220) crystal planes of the spinel Cu (PDF# 04-0836), and the peaks located at 37.0, 42.6, 62.4, and 74.4°, corresponding to (111), (200), (220), and (311) crystal planes of the spinel Cu2O (PDF# 34-1354). Obviously, no other diffraction peaks appeared.

The surface composition and chemical states of the samples were further explored by XPS, as shown in **Figure 2**. It shows that the main elements of Mn, Fe, Co, and Ni were recorded from the XPS. **Figure 2A** depicts the peaks at 640.9, 642.6, 649.2, 644.1, and 652.7 eV, assigned to two spin–orbit doublets of Mn $2p_{1/2}$ and Mn $2p_{3/2}$ and two shake-up satellite peaks (Guo et al., 2017). **Figure 2B** shows the Fe 2p spectrum consisting of two spin–orbit doublets and two shake-up satellites. The multiple peaks at 713.2, 725.2, 711.0, and 713.1 eV can be assigned to the Fe^{3+} $2p_{1/2}$, Fe^{3+} $2p_{3/2}$, Fe^{2+} $2p_{1/2}$, and Fe^{2+} $2p_{3/2}$, while the shake-up satellite peaks are observed at 718.3 and 733.9 eV (Ge et al., 2018). The high-resolution Co 2p spectrum (**Figure 2C**) displays two major peaks at 781.4 and 797.1 eV, corresponding to Co $2p_{3/2}$ and Co $2p_{1/2}$, respectively (Wang et al., 2021; Tabassum et al., 2019). The Ni 2p XPS spectra can be fitted to four components located at 855.9 and 873.5 eV corresponding to Ni $2p_{3/2}$ and Ni $2p_{1/2}$, as shown in Figure 2D (Wu et al., 2017).

The valence state of the Cu and O elements for all M-Cu (M = Mn, Fe, Co, Ni, and Pt) was studied to establish its potential correlations with the HER and OER activities. It can be seen that compared with the pure copper foam, the valence states of copper and oxygen elements changed obviously after adding other metal elements from **Figure 2**. Three fitting components were found on the surface of the sample by O 1s XPS detection: lattice oxygen, surface oxygen species, and oxygen vacancies at the respective energies of ~530.6, 532.3, and 531.3 eV (Kuznetsov et al., 2020)' (Banger et al., 2011). However, for the Cu 2p spectrum, which consists of two spin–orbit doublets and two shake-up satellites, the multiple peaks at 932.9, 934.7, 952.4, and 954.8 eV can be assigned to the Cu^+ $2p_{3/2}$, Cu^{2+} $2p_{3/2}$, Cu^+ $2p_{1/2}$, and Cu^{2+} $2p_{1/2}$, respectively (Chauhan et al., 2017; Zhang et al., 2019b), while the shake-up satellite peaks are observed at 934.0 and 962.5 eV. After the addition of the second metal ion, the second metal ion will be doped into Cu_2O, which may change the lattice parameters, resulting in the shift of the peaks. This indicates that the strong electronic interaction between the cations and the second metal ion leads to electron accumulation around Cu centers (Yan et al., 2021). And for O 1s, the addition of the second metal ion results in the positive shift of the peaks. This indicates that different oxygen vacancy concentrations existed in M-Cu samples (Kuznetsov et al., 2020). Obviously, with the addition of the second metal ion, the valence states of copper and oxygen are changed in different degrees, which will have different degrees of influence on the HER and OER performances.

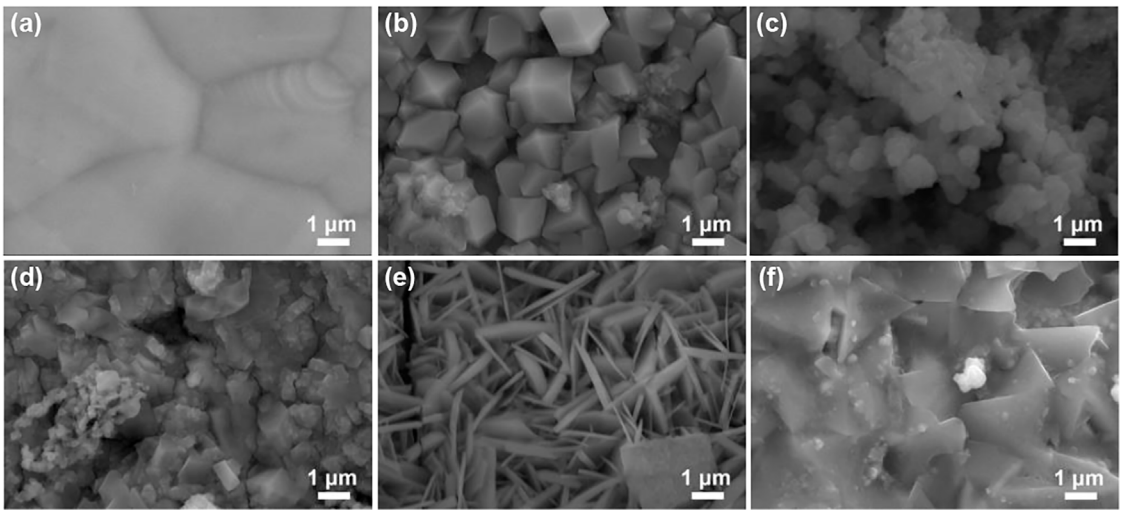

FIGURE 1 | SEM images of **(A)** Cu foam, **(B)** Mn–Cu, **(C)** Fe–Cu, **(D)** Co–Cu, **(E)** Ni–Cu, and **(F)** Pt–Cu.

The HER and OER performances of M-Cu (M = Mn, Fe, Co, Ni, and Pt) samples were measured in 1 M KOH solution using a conventional three-electrode electrochemical setup. By contrast, the HER and OER performances of Cu foam have been tested and are shown in **Supplementary Figure S3**. The overpotentials for the Cu foam at a current density of 10 mA/cm^2 were 728.0 mV for OER and 438.1 mV for HER in 1 M KOH. The higher OER catalytic efficiency is observed on the Co–Cu with a low overpotential of 207.0 mV at 10 mA/cm^2, as evident in **Figure 3A**, smaller than Fe–Cu: 256.8 mV, Ni–Cu: 309.8 mV, and Mn–Cu: 403.2 mV. The excellent kinetic performance of Co–Cu can be proved by its smallest Tafel slope of 56.1 mV/dec (**Figure 3B**). As depicted in **Figure 3C**, it can be found that the HER activity is also with a low overpotential of 215.8 mV at 10 mA/cm^2 for the Fe–Cu sample and 329.8 mV at 10 mA/cm^2 for the Co–Cu sample. The excellent electrochemical performance of all samples can be attributed to the improvement of fast charge transfer kinetics (Yan et al., 2022), so electrochemical impedance spectroscopy (EIS) as a further research was carried out. As shown in **Figure 3D**, the charge transfer resistance of Co–Cu is also significantly smaller, illustrating the small electrode polarization and better electrochemical kinetics. In order to explore the stability of the obtained samples, the chronoamperometric HER test is conducted in **Supplementary Figure S4**. The steady curves obtained at -10 mA cm^{-2} suggest the stable hydrogen evolution behaviors. Additionally, we have added the electrochemical active area (ECSA) tests for the samples (**Supplementary Figure S5**), through the following equation (Voiry et al., 2018):

$$\mathrm{ECSA} = C_{dl}/C_s$$

where C_{dl} represents the electrical double-layer capacitance of the corresponding catalyst and C_s represents the specific capacitance of smooth oxide in 1 M KOH, which is about 0.04 mF/cm^2.

The calculated double-layer capacitance results of Co–Cu, Fe–Cu, Ni–Cu, and Mn–Cu were 20.3, 11.7, 13.4, and 18.7 mF cm^{-2}, respectively. We have also standardized the polarization curves into TOF as follows (Zhang et al., 2017c):

TOF_{O2} = |J| * mA/ECSA * 1 C s^{-1}/1000 mA * 1 mol e$^-$/ 96,495.3 C * 1 mol O_2/4 mol e$^-$ * 6.022 * 10^{23} O_2 molecules/ 1 mol O_2

= |J|/ECSA * 1.56*10^{15} O_2 s^{-1} per mA/cm^2

The calculated results are shown in **Supplementary Figure S6** as follows: in the overpotential of 300 mV, TOF values of Co–Cu, Fe–Cu, Ni–Cu, and Mn-Cu were 1.928*10^{15}, 0.516*10^{15}, 0.079*10^{15}, and 0.002*10^{15} O_2 s^{-1} per mA/cm^2, respectively.

Further insights into the morphology and structure of the as-prepared Pt–Cu products were elucidated by TEM and HRTEM. The (111) planes of Pt were observed in the HRTEM images of **Figure 4B**. Distribution of elements across Pt–Cu was analyzed using the high-resolution EDX elemental mapping analysis in transmission electron microscope (TEM). These EDX maps (**Figure 4C**) confirm the uniform distribution of Pt, Cu, and O across the sample. The Pt 4f peak (**Supplementary Figure S7**) could be separated into two peaks: 75.1 and 77.5 eV, representing the Pt $4f_{5/2}$ and Pt $4f_{7/2}$, respectively (Han et al., 2020). Moreover, when it comes to precious metal Pt, the high OER and HER catalytic efficiencies are observed on the Pt–Cu, as evident in **Figures 4D,E**.

CONCLUSION

In summary, we have synthesized the M-Cu (M = Mn, Fe, Co, Ni, and Pt) samples by a facile method on a copper foam substrate. The electrode shows good HER and OER performances. For non-precious metal, the overpotentials for the Co–Cu sample at a current density of 10 mA/cm^2 were 207.0 mV for OER and 329.8 mV for HER in 1 M KOH solution. Moreover, when adding precious metal Pt,

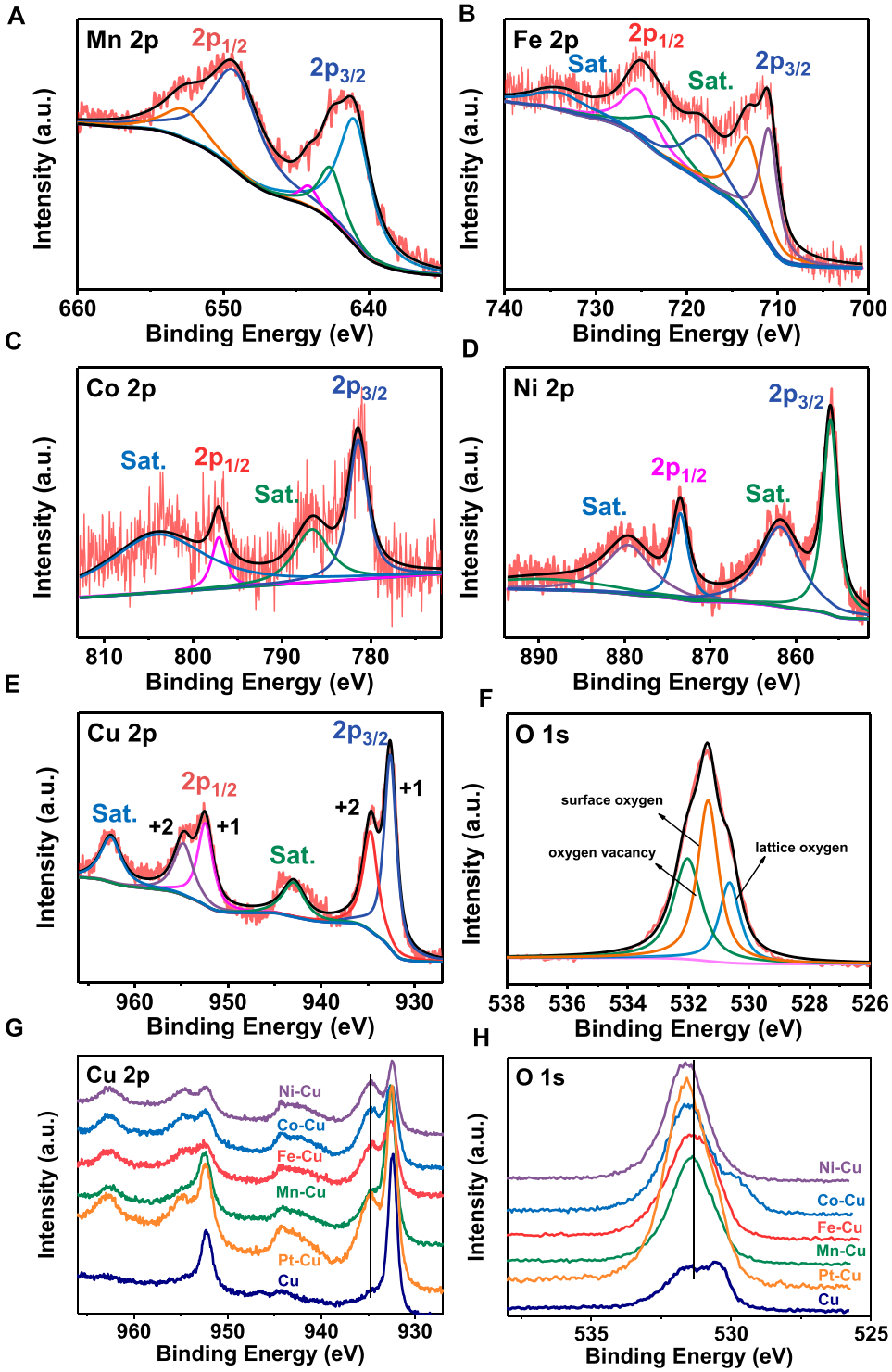

FIGURE 2 | XPS spectra of **(A)** Mn 2p for Mn–Cu, **(B)** Fe 2p for Fe–Cu, **(C)** Co 2p for Co–Cu, **(D)** Ni 2p for Ni–Cu and XPS spectra of **(E)** Cu 2p and **(F)** O 1s for Pt–Cu, **(G)** Cu 2p and **(H)** O 1s for all M-Cu samples.

the high OER and HER catalytic efficiencies were also observed in the Pt–Cu sample. The good HER and OER performances come from the introduction of the second ions, which change the valence states of copper and oxygen elements, resulting in the change of electronic structure of the materials, thus changing its catalytic activity.

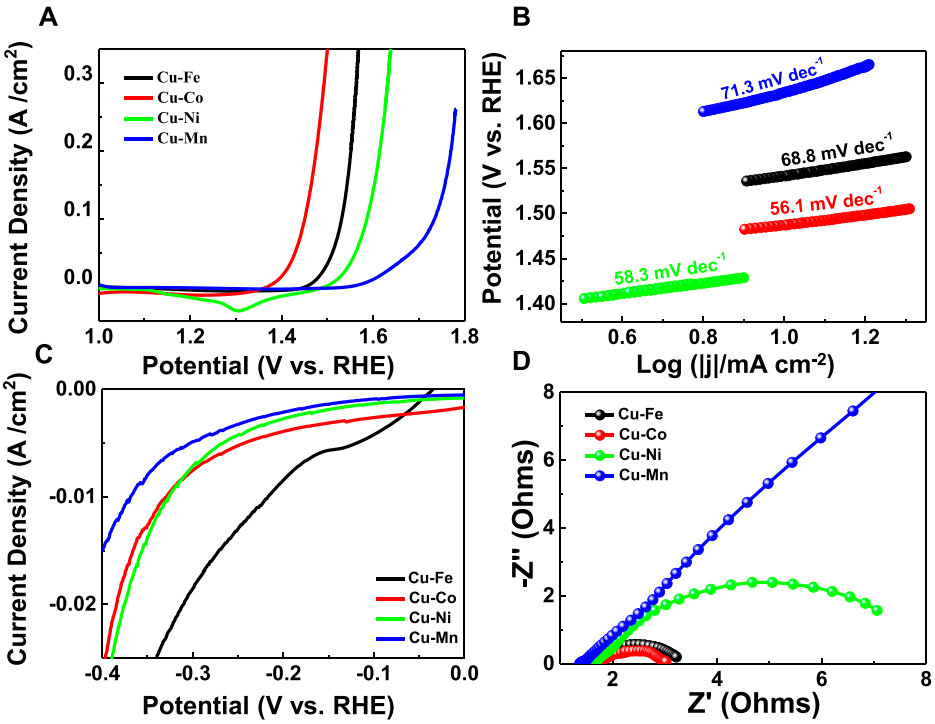

FIGURE 3 | (A) LSV curves and **(B)** Tafel plots of the obtained catalysts for HER tests. **(C)** LSV curves of the obtained catalysts for OER tests. **(D)** Nyquist plots of the obtained catalysts.

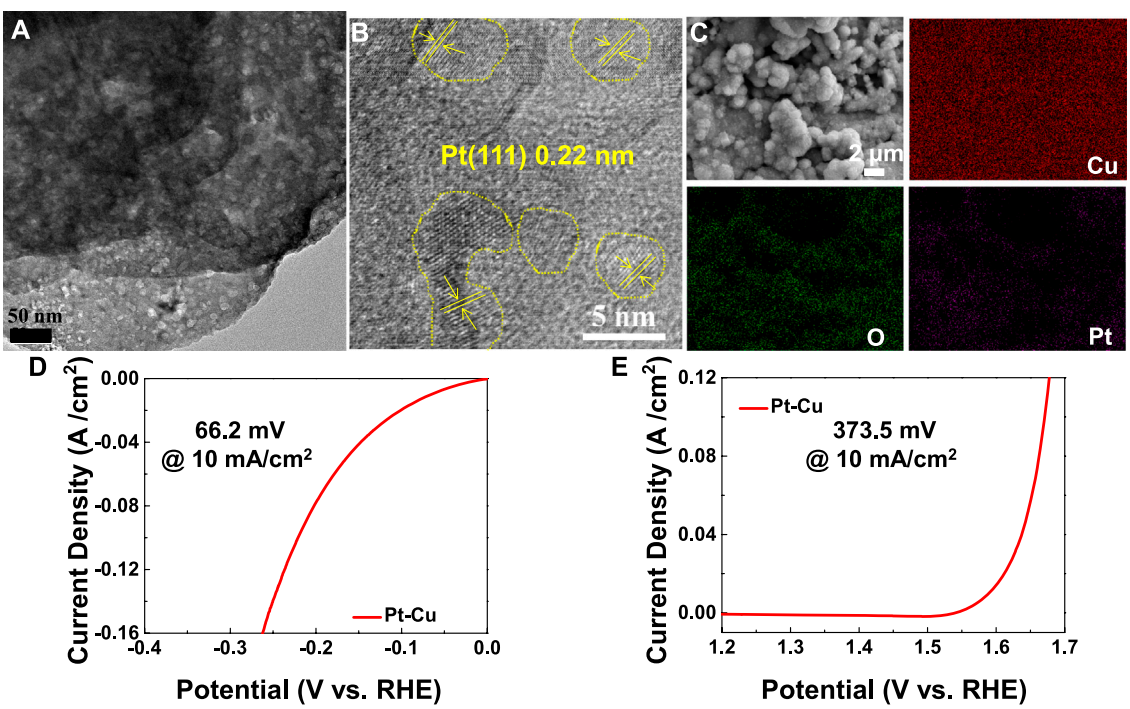

FIGURE 4 | (A) TEM image and **(B)** HRTEM image of Pt–Cu. **(C)** Element mapping of Pt–Cu. LSV curves of **(D)** HER tests and **(E)** OER tests for the Pt–Cu sample.

DATA AVAILABILITY STATEMENT

The original contributions presented in the study are included in the article/**Supplementary Material**; further inquiries can be directed to the corresponding author.

AUTHOR CONTRIBUTIONS

PW: Conceptualization, Methodology, Writing—original draft, Writing—review and editing. JA: Data curation, Writing—review and editing. ZY: Supervision. WC: Supervision, Funding acquisition. XZ: Supervision, Funding acquisition.

FUNDING

PW and JA contributed equally to this work. The support from the National Natural Science Foundation of China (No. 51971083) and the Natural Science Foundation of Heilongjiang Province, China (YQ 2020E007) is gratefully acknowledged. This work was financially sponsored by Heilongjiang Touyan Team Program.

SUPPLEMENTARY MATERIAL

The Supplementary Material for this article can be found online at: https://www.frontiersin.org/articles/10.3389/fchem.2022.913874/full#supplementary-material

REFERENCES

Anandhababu, G., Huang, Y., Babu, D. D., Wu, M., and Wang, Y. (2018). Oriented Growth of ZIF-67 to Derive 2D Porous CoPO Nanosheets for Electrochemical-/Photovoltage-Driven Overall Water Splitting. *Adv. Funct. Mat.* 28, 6120. doi:10.1002/adfm.201706120

Banger, K. K., Yamashita, Y., Mori, K., Peterson, R. L., Leedham, T., Rickard, J., et al. (2011). Low-temperature, High-Performance Solution-Processed Metal Oxide Thin-Film Transistors Formed by a 'sol-Gel on Chip' Process. *Nat. Mater* 10, 45–50. doi:10.1038/nmat2914

Chauhan, M., Reddy, K. P., Gopinath, C. S., and Deka, S. (2017). Copper Cobalt Sulfide Nanosheets Realizing a Promising Electrocatalytic Oxygen Evolution Reaction. *ACS Catal.* 7, 5871–5879. doi:10.1021/acscatal.7b01831

Gatalo, M., Moriau, L., Petek, U., Ruiz-Zepeda, F., Šala, M., Grom, M., et al. (2019). CO-assisted *Ex-Situ* Chemical Activation of Pt-Cu/C Oxygen Reduction Reaction Electrocatalyst. *Electrochimica Acta* 306, 377–386. doi:10.1016/j.electacta.2019.03.153

Ge, P., Hou, H., Li, S., Yang, L., and Ji, X. (2018). Tailoring Rod-like FeSe2 Coated with Nitrogen-Doped Carbon for High-Performance Sodium Storage. *Adv. Funct. Mat.* 28. doi:10.1002/adfm.201801765

Guo, X. L., Zhang, J. M., Xu, W. N., Hu, C. G., Sun, L., and Zhang, Y. X. (2017). Growth of NiMn LDH Nanosheet Arrays on KCu7S4 Microwires for Hybrid Supercapacitors with Enhanced Electrochemical Performance. *J. Mat. Chem. A* 5, 20579–20587. doi:10.1039/c7ta04382a

Han, Z., Zhang, R.-L., Duan, J.-J., Wang, A.-J., Zhang, Q.-L., Huang, H., et al. (2020). Platinum-rhodium Alloyed Dendritic Nanoassemblies: An All-pH Efficient and Stable Electrocatalyst for Hydrogen Evolution Reaction. *Int. J. Hydrogen Energy* 45, 6110–6119. doi:10.1016/j.ijhydene.2019.12.155

Jebaslinhepzybai, B. T., Partheeban, T., Gavali, D. S., Thapa, R., and Sasidharan, M. (2021). One-pot Solvothermal Synthesis of Co2P Nanoparticles: An Efficient HER and OER Electrocatalysts. *Int. J. Hydrogen Energy* 46, 21924–21938. doi:10.1016/j.ijhydene.2021.04.022

Kim, J., Jung, H., Jung, S.-M., Hwang, J., Kim, D. Y., Lee, N., et al. (2021). Tailoring Binding Abilities by Incorporating Oxophilic Transition Metals on 3D Nanostructured Ni Arrays for Accelerated Alkaline Hydrogen Evolution Reaction. *J. Am. Chem. Soc.* 143, 1399–1408. doi:10.1021/jacs.0c10661

Koh, S., and Strasser, P. (2007). Electrocatalysis on Bimetallic Surfaces: Modifying Catalytic Reactivity for Oxygen Reduction by Voltammetric Surface Dealloying. *J. Am. Chem. Soc.* 129, 12624–12625. doi:10.1021/ja0742784

Kuznetsov, D. A., Naeem, M. A., Kumar, P. V., Abdala, P. M., Fedorov, A., and Müller, C. R. (2020). Tailoring Lattice Oxygen Binding in Ruthenium Pyrochlores to Enhance Oxygen Evolution Activity. *J. Am. Chem. Soc.* 142, 7883–7888. doi:10.1021/jacs.0c01135

Lee, S. Y., Jung, H., Kim, N.-K., Oh, H.-S., Min, B. K., and Hwang, Y. J. (2018). Mixed Copper States in Anodized Cu Electrocatalyst for Stable and Selective Ethylene Production from CO2 Reduction. *J. Am. Chem. Soc.* 140, 8681–8689. doi:10.1021/jacs.8b02173

Li, D. Y., Liao, L. L., Zhou, H. Q., Zhao, Y., Cai, F. M., Zeng, J. S., et al. (2021). Highly Active Non-noble Electrocatalyst from Co2P/Ni2P Nanohybrids for pH-Universal Hydrogen Evolution Reaction. *Mater. TODAY Phys.* 16, 314. doi:10.1016/j.mtphys.2020.100314

Li, K., Li, Y., Wang, Y., Ge, J., Liu, C., and Xing, W. (2018). Enhanced Electrocatalytic Performance for the Hydrogen Evolution Reaction through Surface Enrichment of Platinum Nanoclusters Alloying with Ruthenium *In Situ* Embedded in Carbon. *Energy Environ. Sci.* 11, 1232–1239. doi:10.1039/c8ee00402a

Liu, Z., Qiu, Y., Zhang, A., Yang, W., Barrow, C. J., Razal, J. M., et al. (2021). *In Situ* embedding of Cobalt Sulfide Quantum Dots Among Transition Metal Layered Double Hydroxides for High Performance All-Solid-State Asymmetric Supercapacitors. *J. Mat. Chem. A* 9, 22573–22584. doi:10.1039/d1ta06706k

Qiu, Y., Xie, X., Li, W., and Shao, Y. (2021). Electrocatalysts Development for Hydrogen Oxidation Reaction in Alkaline Media: From Mechanism Understanding to Materials Design. *Chin. J. Catal.* 42, 2094–2104. doi:10.1016/s1872-2067(21)64088-3

Sultan, S., Tiwari, J. N., Singh, A. N., Zhumagali, S., Ha, M., Myung, C. W., et al. (2019). Single Atoms and Clusters Based Nanomaterials for Hydrogen Evolution, Oxygen Evolution Reactions, and Full Water Splitting. *Adv. Energy Mat.* 9, 1900624. doi:10.1002/aenm.201900624

Tabassum, H., Zhi, C., Hussain, T., Qiu, T., Aftab, W., and Zou, R. (2019). Encapsulating Trogtalite CoSe2 Nanobuds into BCN Nanotubes as High Storage Capacity Sodium Ion Battery Anodes. *Adv. Energy Mat.* 9. doi:10.1002/aenm.201901778

Tomboc, G. M., Choi, S., Kwon, T., Hwang, Y. J., and Lee, K. (2020). Potential Link between Cu Surface and Selective CO2 Electroreduction: Perspective on Future Electrocatalyst Designs. *Adv. Mat.* 32, e1908398. doi:10.1002/adma.201908398

Voiry, D., Chhowalla, M., Gogotsi, Y., Kotov, N. A., Li, Y., Penner, R. M., et al. (2018). Best Practices for Reporting Electrocatalytic Performance of Nanomaterials. *ACS Nano* 12, 9635–9638. doi:10.1021/acsnano.8b07700

Wang, P., Huang, J., Zhang, J., Wang, L., Sun, P., Yang, Y., et al. (2021). Coupling Hierarchical Iron Cobalt Selenide Arrays with N-Doped Carbon as Advanced Anodes for Sodium Ion Storage. *J. Mat. Chem. A* 9, 7248–7256. doi:10.1039/d1ta00226k

Wu, D., Kusada, K., Yamamoto, T., Toriyama, T., Matsumura, S., Gueye, I., et al. (2021). Correction: On the Electronic Structure and Hydrogen Evolution Reaction Activity of Platinum Group Metal-Based High-Entropy-Alloy Nanoparticles. *Chem. Sci.* 12, 7196. doi:10.1039/d1sc90104d

Wu, P., Cheng, S., Yao, M., Yang, L., Zhu, Y., Liu, P., et al. (2017). A Low-Cost, Self-Standing NiCo2O4@CNT/CNT Multilayer Electrode for Flexible Asymmetric Solid-State Supercapacitors. *Adv. Funct. Mat.* 27. doi:10.1002/adfm.201702160

Yan, Y., Bao, K., Liu, T., Cao, J., Feng, J., and Qi, J. (2020). Minutes Periodic Wet Chemistry Engineering to Turn Bulk Co-ni Foam into Hydroxide Based Nanosheets for Efficient Water Decomposition. *Chem. Eng. J.* 401, 126092. doi:10.1016/j.cej.2020.126092

Yan, Y., Lin, J., Liu, T., Liu, B., Wang, B., Qiao, L., et al. (2022). Corrosion Behavior of Stainless Steel-Tungsten Carbide Joints Brazed with AgCuX (X = in, Ti) Alloys. *Corros. Sci.* 200, 110231. doi:10.1016/j.corsci.2022.110231

Yan, Y., Liu, J., Huang, K., Qi, J., Qiao, L., Zheng, X., et al. (2021). A Fast Micro-nano Liquid Layer Induced Construction of Scaled-Up Oxyhydroxide Based

Electrocatalysts for Alkaline Water Splitting. *J. Mat. Chem. A* 9, 26777–26787. doi:10.1039/d1ta07972g

Yang, M., Jiao, L., Dong, H., Zhou, L., Teng, C., Yan, D., et al. (2021). Conversion of Bimetallic MOF to Ru-Doped Cu Electrocatalysts for Efficient Hydrogen Evolution in Alkaline Media. *Sci. Bull.* 66, 257–264. doi:10.1016/j.scib.2020.06.036

Yang, W., and Chen, S. (2020). Recent Progress in Electrode Fabrication for Electrocatalytic Hydrogen Evolution Reaction: A Mini Review. *Chem. Eng. J.* 393, 124726. doi:10.1016/j.cej.2020.124726

Yuan, H., Wang, S., Ma, Z., Kundu, M., Tang, B., Li, J., et al. (2021). Oxygen Vacancies Engineered Self-Supported B Doped Co3O4 Nanowires as an Efficient Multifunctional Catalyst for Electrochemical Water Splitting and Hydrolysis of Sodium Borohydride. *Chem. Eng. J.* 404, 126474. doi:10.1016/j.cej.2020.126474

Zhang, A., Zheng, W., Yuan, Z., Tian, J., Yue, L., Zheng, R., et al. (2020). Hierarchical NiMn-Layered Double hydroxides@CuO Core-Shell Heterostructure *In-Situ* Generated on Cu(OH)(2) Nanorod Arrays for High Performance Supercapacitors. *Chem. Eng. J.* 380, 122486. doi:10.1016/j.cej.2019.122486

Zhang, B., Lui, Y. H., Zhou, L., Tang, X., and Hu, S. (2017). An Alkaline Electro-Activated Fe-Ni Phosphide Nanoparticle-Stack Array for High-Performance Oxygen Evolution under Alkaline and Neutral Conditions. *J. Mat. Chem. A* 5, 13329–13335. doi:10.1039/c7ta03163g

Zhang, J., Wang, T., Liu, P., Liao, Z., Liu, S., Zhuang, X., et al. (2017). Efficient Hydrogen Production on MoNi4 Electrocatalysts with Fast Water Dissociation Kinetics. *Nat. Commun.* 8, 15437. doi:10.1038/ncomms15437

Zhang, J., Zhang, Q., and Feng, X. (2019). Support and Interface Effects in Water-Splitting Electrocatalysts. *Adv. Mat.* 31, e1808167. doi:10.1002/adma.201808167

Zhang, J., Zhang, Z., Ji, Y., Yang, J., Fan, K., Ma, X., et al. (2021). Surface Engineering Induced Hierarchical Porous Ni12P5-Ni2P Polymorphs Catalyst for Efficient Wide pH Hydrogen Production. *Appl. Catal. B-Environ.* 282, 119609. doi:10.1016/j.apcatb.2020.119609

Zhang, S., Zhao, C., Liu, Y., Li, W., Wang, J., Wang, G., et al. (2019). Cu Doping in CeO2 to Form Multiple Oxygen Vacancies for Dramatically Enhanced Ambient N2 Reduction Performance. *Chem. Commun.* 55, 2952–2955. doi:10.1039/c9cc00123a

Zhang, Y., Liu, Y., Ma, M., Ren, X., Liu, Z., Du, G., et al. (2017). A Mn-Doped Ni2P Nanosheet Array: an Efficient and Durable Hydrogen Evolution Reaction Electrocatalyst in Alkaline Media. *Chem. Commun.* 53, 11048–11051. doi:10.1039/c7cc06278h

Zhou, H., Yu, F., Zhu, Q., Sun, J., Qin, F., Yu, L., et al. (2018). Water Splitting by Electrolysis at High Current Densities under 1.6 Volts. *Energy Environ. Sci.* 11, 2858–2864. doi:10.1039/c8ee00927a

Zhu, W., Zhang, R., Qu, F., Asiri, A. M., and Sun, X. (2017). Design and Application of Foams for Electrocatalysis. *ChemCatChem* 9, 1721–1743. doi:10.1002/cctc.201601607

Zhu, Y., Zhang, L., Zhang, X., Li, Z., Zha, M., Li, M., et al. (2021). Double Functionalization Strategy toward Co-fe-P Hollow Nanocubes for Highly Efficient Overall Water Splitting with Ultra-low Cell Voltage. *Chem. Eng. J.* 405, 127002. doi:10.1016/j.cej.2020.127002

Conflict of Interest: The authors declare that the research was conducted in the absence of any commercial or financial relationships that could be construed as a potential conflict of interest.

Publisher's Note: All claims expressed in this article are solely those of the authors and do not necessarily represent those of their affiliated organizations, or those of the publisher, the editors, and the reviewers. Any product that may be evaluated in this article, or claim that may be made by its manufacturer, is not guaranteed or endorsed by the publisher.